Eur. Phys. J. B **4**, 147–157 (1998)

THE EUROPEAN PHYSICAL JOURNAL B

Filling carbon nanotubes with metals by the arc-discharge method: the key role of sulfur

N. Demoncy[1,2], O. Stéphan[3], N. Brun[3], C. Colliex[3,4], A. Loiseau[2,a], and H. Pascard[1]

[1] Laboratoire des Solides Irradiés, CEA-CNRS, École Polytechnique, 91128 Palaiseau Cedex, France
[2] Laboratoire d'Étude des Microstructures, ONERA-CNRS, Office National d'Études et de Recherches Aérospatiales, BP 72, 92322 Châtillon Cedex, France
[3] Laboratoire de Physique des Solides[b], Université de Paris-Sud, Bâtiment 510, 91405 Orsay Cedex, France
[4] Laboratoire Aimé Cotton[c], Campus d'Orsay, Bâtiment 505, 91405 Orsay Cedex, France

Received: 20 January 1998 / Received in final form and accepted: 9 April 1998

Abstract. Various filled carbon nanotubes have recently been successfully produced by the arc-discharge method by doping a 99.4% graphite anode with a transition metal like Cr, Ni, a rare earth like Yb, Dy, or a covalent element like S, Ge. In this work, the structural characteristics of these encapsulated nanowires were studied by High Resolution Transmission Electron Microscopy and their chemical composition was investigated using Electron Energy-Loss Spectroscopy with high spatial resolution: this analysis mode provides elemental concentration profiles across or along the filled nanotubes. Except in the case of Ge for which only pure Ge fillings were identified, surprising amounts of sulfur, which was present as an impurity ($\approx 0.25\%$) in the graphite rods, were found within numerous filling materials. When using high purity carbon rods, no filled nanotube was obtained. We chose the case of Cr to clearly evidence that the addition of sulfur in catalytic quantity is responsible for the formation of filled nanotubes, including sulfur free encapsulated nanowires. A growth mechanism based on a catalytic process involving three elements, *i.e.* carbon, a metal and sulfur, and taking into account the experimental results is proposed.

PACS. 61.16.Bg Transmission, reflection and scanning electron microscopy (including EBIC) – 81.05.Tp Fullerenes and related materials; diamonds, graphite

1 Introduction

The discovery of carbon nanotubes by Iijima [1] led to an extensive interest motivated by the prediction of specific properties and in particular of an unique capillary behaviour [2]. Ajayan *et al.* succeeded in opening and filling carbon nanotubes by heating them in air in presence of molten Pb [3]. Various materials have since been inserted into nanotubes using different methods. Specific electronic, magnetic or mechanical properties can be expected for these one-dimensional encapsulated nanomaterials. Measurements of individual physical properties of such nano-objects have recently been achieved [4,5]. Although the potential applications of filled nanotubes in nanotechnology are for the moment speculative, the production and purification of encapsulated nanowires having controlled structural and chemical characteristics will probably be required in a near future.

The first route to produce filled carbon nanotubes is to use pre-existing nanotubes and to fill them by different techniques. First, molten media have been used to fill nanotubes with compounds having low surface tension [6]: beside PbO, compounds like Bi_2O_3 [7], V_2O_5 [8], MoO_3 [9] or $AgNO_3$ [10], have been inserted by capillarity through open ends. An other way to fill pre-existing nanotubes involves wet chemistry solution methods [11,12]. In that case, the metal oxides or metals that are encapsulated are discrete crystals unlike the long continuous fillings obtained by molten media or arc-discharge as described below. Finally, it is also interesting to mention that carbon nanotubes have been converted to carbide nanorods, which are not encapsulated, by reaction with oxide or iodide species [13].

The second route is to produce the nanotubes and their fillings simultaneously. Recently, encapsulated Sn nanowires have been obtained by electrolysis of graphite electrodes immersed in molten $LiCl/SnCl_2$ mixtures [14]. But filled nanotubes have mostly been synthesized using a modified arc-discharge method in which the anode is doped with a chosen compound. The arc-discharge method, which consists in establishing an electric arc between two graphite electrodes in a He atmosphere, was first used by Krätschmer *et al.* to produce fullerenes in large quantities [15] and was later optimized for

[a] e-mail: loiseau@onera.fr
[b] CNRS URA 002
[c] CNRS UPR 3321

the synthesis of carbon nanotubes [1,16]. The modified arc-discharge method led to the formation of endohedral fullerenes [17] and then of nanoparticles encapsulated in graphitic shells [18,19]. The first filled nanotubes produced by this method contained yttrium carbide [20–22]. Other carbides (Gd, La, Mn) were later inserted into nanotubes by the same method [23–25]. As far as nanotubes filled with pure elements are concerned, partial fillings of pure Ni inside bamboo-shape carbon nanotubes have first been reported [26]. In 1994, Ajayan *et al.* showed that long pure Mn fillings can be formed by doping the anode with pure Mn metal [27] and recently, pure Cu and Ge nanowires have been synthesized using a hydrogen arc [28,29]. As previously reported [30–32], we succeeded in synthesizing various filled nanotubes by successively doping the anode with several elements. Long continuous fillings, often exceeding one micron in length and therefore being true encapsulated nanowires, were obtained for ten elements belonging to different groups: transition metals (Cr, Ni), rare earths (Sm, Gd, Dy, Yb) and covalent elements (S, Ge, Se, Sb). Partial fillings were also obtained with elements like Co, Fe and Pd. The fillings were generally found to be compounds, except in a few cases like Ge for which the nanowires were pure Ge crystals encapsulated in a few graphitic layers.

In this work, we studied in detail both the structure and the chemical composition of these encapsulated nanowires using High Resolution Transmission Electron Microscopy (HRTEM) and high spatial resolution Electron Energy Loss Spectroscopy (EELS). Here we show how this investigation revealed that the successful formation of carbon nanotubes filled with metals by arc-discharge relies on the presence of a small amount of sulfur, which was initially present as an impurity in the graphite electrodes. A particular attention was paid to the case of Cr to clearly evidence that sulfur is responsible for the growth of filled nanotubes, including free from sulfur encapsulated nanowires. The key role of sulfur in the formation of filled nanotubes is finally discussed and a growth mechanism taking into account the experimental results is proposed.

2 Experimental conditions

Several elements of the periodic table have been tested [30,31] for filling carbon nanotubes by the arc-discharge method using the experimental conditions described in reference [30]. In brief, we used two graphite electrodes (purity 99.4%) 9 mm in diameter. The anode was drilled with a 6-mm hole and packed with a mixture of graphite and chosen element powders. The arcing conditions were 100-110 A dc, 20-30 V, under a 0.6 bar He atmosphere, during 30-60 min. The deposit formed on the cathode and containing filled nanotubes and nanoparticles encapsulated in graphitic shells was ground, ultrasonically dispersed in ethanol and dropped on holey carbon grids for electron microscopy observations.

HRTEM and standard EELS characterizations were performed using a JEOL 4000FX working at 400 kV, equipped with a Gatan 666 parallel collection electron

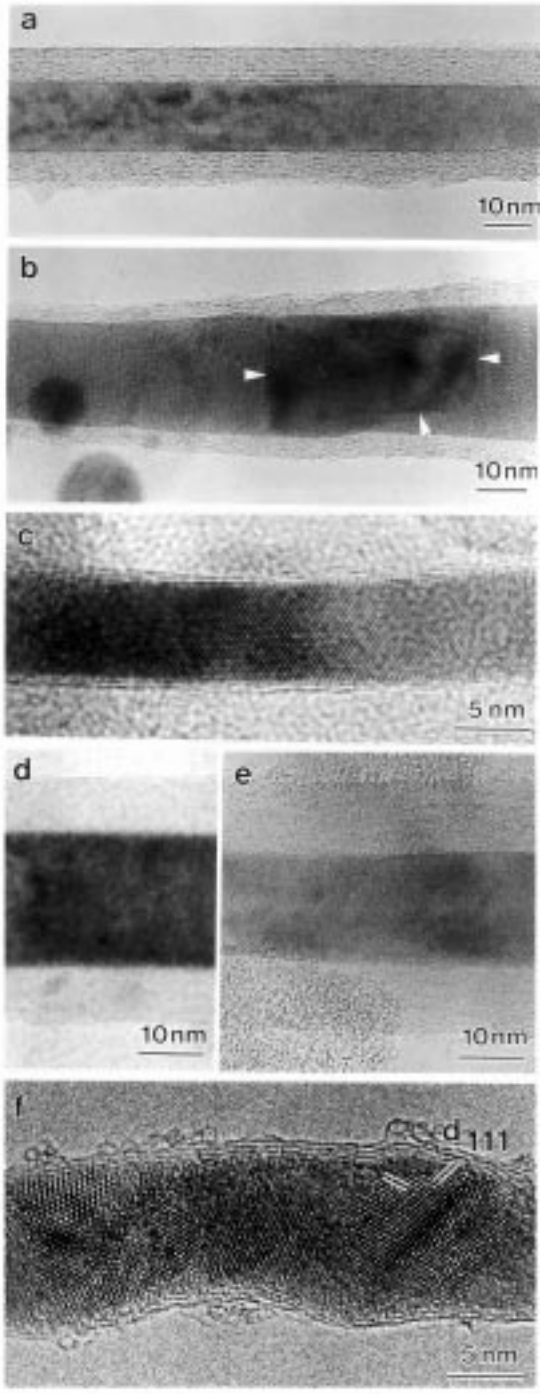

Fig. 1. HRTEM images of filled carbon nanotubes produced by arc-discharge when a 99.4% graphite anode is doped with: (a) Cr, (b) Ni, (c) Yb, (d) Dy, (e) S, (f) Ge. The graphitic walls of the nanotubes are imaged by fringes separated by approximately 0.34 nm. In the case of Ni (b), white arrows indicate grain boundaries present in the filling material. In the case of Ge (f), the filling material is polycrystalline and encapsulated in only 2 or 3 graphitic layers. Pure Ge microcrystals in a ⟨110⟩ projection can be seen on the left and right parts of the nanowire and typical microtwins and stacking faults of the ⟨111⟩ dense atomic layers are frequently observed.

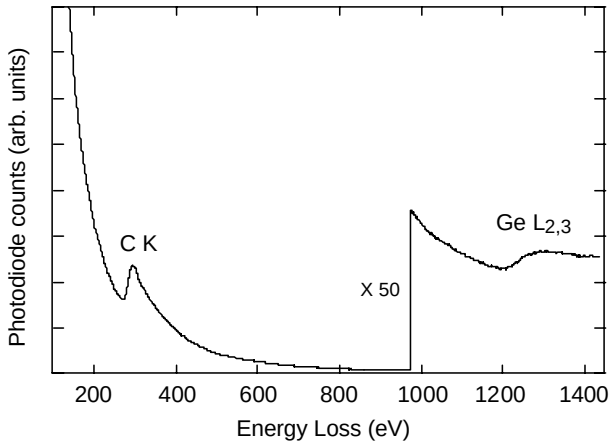

Fig. 2. Electron energy-loss spectrum obtained on a part of a pure Ge nanowire encapsulated in graphitic walls. The C-K and Ge-$L_{2,3}$ edges are clearly seen and no other edge is detected.

energy-loss spectrometer. High spatial resolution EELS analyses were performed using a dedicated scanning transmission electron microscope (STEM) VG HB501, working at 100 kV, equipped with a field-emission source and a parallel collection electron energy-loss spectrometer. This instrument provides EELS spectra with a typical 0.7 eV resolution recorded on subnanometer areas. Acquisition times required for achieving a satisfactory signal to noise level on core-loss signals is of the order of 1 s. An annular dark field detector collects electrons scattered at large angles; annular dark field images are obtained by rastering the subnanometer probe over a scan area. In the usual mode, one rasters the probe over a reduced area while recording annular dark field image so that a location of the specimen can be chosen for acquiring the corresponding EELS spectrum. A new mode, called line-spectrum mode [33], improves the correlation between spectral acquisition and the probe position on the specimen. It consists in recording all the spectra while ramping the probe at given steps across the specimen. Typically, in this work we acquired collections of 64 spectra with subnanometer step increments, a probe size of 1 nm and an acquisition time per spectrum of 1 s. The intensity profiles of the core-edges after background substraction follow the thickness profiles. Quantitative features, *i.e.* relative atomic concentration profiles, can be obtained by normalizing the intensity profiles with the inelastic scattering cross-sections respective to each edge. We have generally scanned the probe perpendicularly to the tube axis, moving the probe from vacuum into the nanotube and to vacuum again. The intensity profile perpendicularly to a hollow carbon nanotube has a typical shape [34]: as the beam scans across, the intensity increases up to a probe position which corresponds roughly to the location of the internal wall, then dips in the middle due to the hollow core (the minimum of intensity occurs for a probe location corresponding to the center of the nanotube) and exhibits a symmetrical behaviour on the opposite side (see for instance C profile in Fig. 3b). Note that longitudinal line-scans can also be obtained by scanning the electron beam along the tube axis.

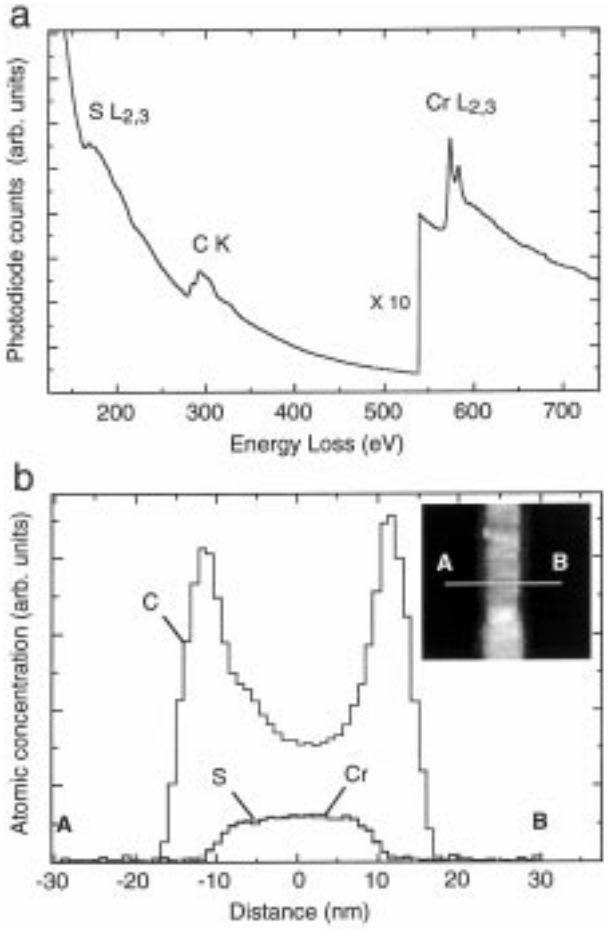

Fig. 3. Electron energy-loss line-spectrum across a filled carbon nanotube obtained with a 99.4% graphite anode doped with Cr. A collection of 64 spectra was acquired over 60 nm perpendicularly to the tube axis. (a) Sum of spectra obtained on the filled part of the nanotube showing the C-K, Cr-$L_{2,3}$ edges and the unexpected S-$L_{2,3}$ edge. (b) Concentration profiles deduced from the intensities of the C-K, Cr-$L_{2,3}$ and S-$L_{2,3}$ edges as the beam is scanned across the filled nanotube. The C profile is characteristic of a carbon nanotube, whose hollow core is filled with a chromium sulfide as shown by the well-correlated Cr and S profiles. The S/Cr atomic ratio is close to 1. Inset: Annular dark field image of the nanowire. The white bar represents the line of scan.

3 Structural and chemical analyses

Figure 1 presents a selection of HRTEM images of filled nanotubes that have been successfully produced when the anode was doped with a transition metal like Cr, Ni (Figs. 1a, b), a rare earth like Yb, Dy (Figs. 1c, d) and a covalent element like S, Ge (Figs. 1e, f). Their structural characteristics, *i.e.* the number of graphitic layers, the degree of graphitization, the crystallinity of the filling material, depend on the chosen element as previously reported [30,31]. The nanotubes are often completely filled from their tips and their length ranges from a few hundred nanometers to a few microns. However for some elements like Co or Fe not presented here (see [30]), only partial

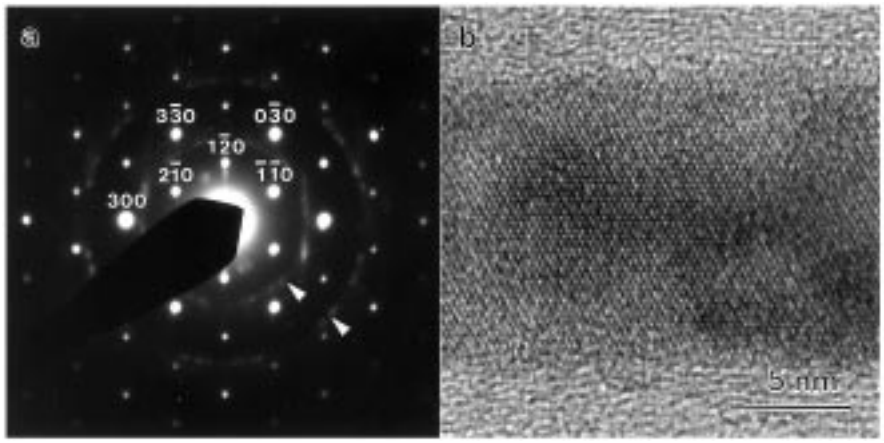

Fig. 4. (a) Selected area electron diffraction pattern of a conveniently oriented nanotube filled with Cr and S consistent with a ⟨001⟩ projection of the trigonal chromium sulfides Cr_5S_6 or Cr_2S_3 (which have the same space group and very close lattice parameters) (b) Corresponding HRTEM image showing the 3.0 Å periodicities due to ⟨110⟩ type reflections. Note that the graphitic layers are very disordered because of irradiation damage in the microscope.

fillings never exceeding a few hundred nanometers have been found.

The encapsulated crystals were initially thought to be carbides since in most cases the corresponding selected area electron diffraction (SAED) patterns were not consistent with the pure elements, except for Ge. In that particular case, the nanotubes are very thin and abundant, generally completely filled from their tips over a few hundred nanometers. It is worth noting that Ge nanowires recently produced using a hydrogen arc are very similar [29]. Figure 1f shows a HRTEM image of a typical 10 nm-diameter nanowire encapsulated in only 2 or 3 graphitic layers. Although long single-crystals have also been observed, the fillings are often polycrystalline as the one presented in Figure 1f. Microcrystallites in ⟨110⟩ projection can be seen on the left and right parts of the nanowire; the distance between the fringes is consistent with the reticular distance of the ⟨111⟩ atomic planes in pure Ge (d_{111} = 3.2 Å). Typical microtwins and stacking faults of the ⟨111⟩ dense atomic layers are frequently observed. The chemical composition was studied by EELS: only the C-K edge (285 eV) and the Ge-$L_{2,3}$ edge (1217 eV) are present on the spectra obtained on selected parts of these nanowires as shown in Figure 2.

Since no stable Ge carbide phase is known, this result is consistent with the HRTEM observations of pure Ge nanocrystals.

The chemical composition of encapsulated nanowires was investigated in a rather systematic way using high spatial resolution EELS. Surprisingly, important amounts of sulfur were found in numerous filling materials along with the inserted element. The source of sulfur was identified to be the used graphite electrodes (purity 99.4%): a refined chemical analysis of the graphite powder showed that the major impurities are Fe (≈ 0.3% in weight with respect to C) and S (≈ 0.25%). The case of Cr containing filled nanotubes is emphasized in Figure 3a: in addition to the C-K edge and Cr-$L_{2,3}$ edge (575 eV), the unexpected S-$L_{2,3}$ edge (165 eV) appears on the EELS spectra for a large number of nanotubes. Figure 3b presents an example of concentration profiles deduced from a line-spectrum across the filled nanotube shown in inset. The C profile is characteristic of a hollow carbon nanotube and the excellent correlation between S and Cr profiles suggests a homogeneous filling of the hollow core: the S and Cr intensities are well anticorrelated to the C intensity. EELS nano-analysis clearly evidenced that such nanotubes are not filled with carbides but with sulfides. The S/Cr atomic ratio is close to 1 ± 0.2. It is worth noting that a precise quantification of the S-$L_{2,3}$ edge is difficult to obtain, especially when the amount of sulfur is close to zero. Indeed, the modelisation of the high slope of the background before the S-$L_{2,3}$ edge is not easy in this energy range not very far from the multiple plasmon-loss region and the calculated inelastic scattering cross-section in the Hartree-Slater approximation does not provide a good modelisation for the delayed shape of the S-$L_{2,3}$ edge. As shown in Figure 1a, long single-crystals are often observed and longitudinal line-spectra confirmed the homogeneous composition over long parts of the nanowires. A particular approach using both EELS analysis and electron diffraction on a given filled nanotube was used to determine both the chemical composition and the lattice structure through a careful analysis of the reciprocal space deduced from SAED patterns obtained for different orientations. For a majority of S containing nanowires, the structure was found to be trigonal and consistent with that of Cr_5S_6, for which the S/Cr atomic ratio is close to 1, or Cr_2S_3. Figure 4 presents the SAED pattern and the corresponding HRTEM image of such a chromium sulfide nanowire in a ⟨001⟩ projection. The arrows show the diffraction spots due to the graphitic nanotubes. It is very interesting to note that the tube axis was always found to be parallel to a ⟨300⟩ direction proving that strong orientational relationships exist between the nanotube and the inner crystal during its formation.

Sulfur was also found inside nanotubes filled with Ni. As for Cr, transverse EELS line-spectra showed that sulfur was homogeneously mixed with nickel inside the nanotubes. However, in constrast with Cr, longitudinal line-spectra revealed that the S/Ni atomic ratio can vary along the tube axis. Two typical examples are presented in Figure 5. S and Ni concentration profiles are well anticorrelated and the resulting S/Ni atomic ratio takes discrete values, namely ≈ 0.4, ≈ 0, ≈ 0.4, ≈ 0 (±0.2)

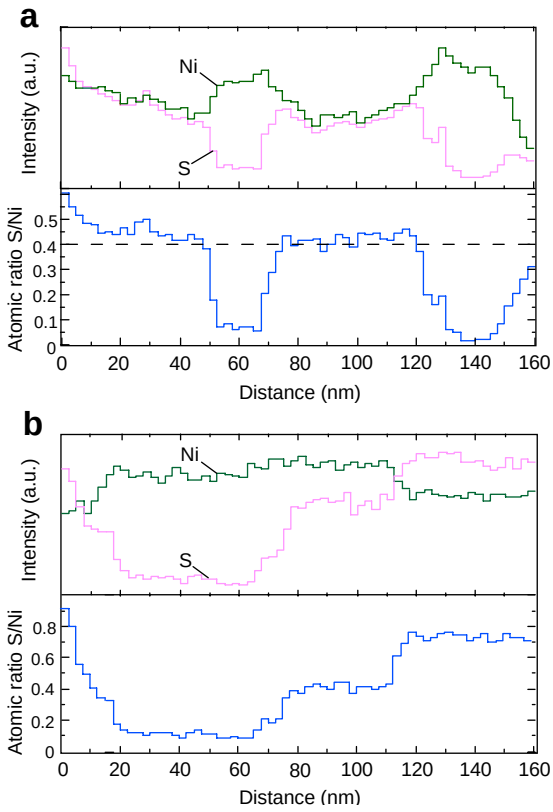

Fig. 5. (a) and (b) Longitudinal electron energy-loss line-spectra along the axis of two filled carbon nanotubes obtained with a 99.4% graphite anode doped with Ni. Collections of 64 spectra were acquired over 160 nm and the Ni and S concentration profiles were deduced from the intensities of the Ni-$L_{2,3}$ and S-$L_{2,3}$ edges. In (a), the S/Ni atomic ratio takes discrete values along the tube axis: ≈ 0.4, ≈ 0, ≈ 0.4, ≈ 0. The filling material is alternatively pure Ni and a nickel sulfide inside this nanotube. In (b), the left part corresponds to a sulfur rich region close to the tip of the nanotube. Then, the S/Ni atomic ratio has a stairs shape, ≈ 0, ≈ 0.4, ≈ 0.7, corresponding to a succession of definite compounds within the filling material.

in Figure 5a: in this nanotube, the filling material is alternatively pure Ni and a nickel sulfide. No stable nickel sulfide corresponding to a S/Ni ratio close to 0.4 is known. Therefore, it is likely that a metastable sulfide has been formed. More important amounts of sulfur were also found, in particular at the tip of nanowires (see the left part of Fig. 5b). It is interesting to note that in some cases, we observed SAED patterns of crystallites conveniently oriented, as those shown in Figure 6, consistent with the α-Ni_3S_2 pseudo-cubic phase. The corresponding S/Ni atomic ratio is close to the 0.7 ratio we observed in some EELS analyses (see Fig. 5b). These results show that various chemical compositions can be found within the same continuous filling, including pure Ni metal and different sulfides. Moreover, composition changes can be related to structural and morphological changes of the filling material observed on HRTEM images. For example in Figure 1b, the filling displays three crystallites having different structures and imaged by different arrays of fringes; the grain boundaries are indicated with arrows on the image.

Sulfide fillings were also obtained with Co but were always partial and often had a conical shape. Figure 7a exhibits an elongated particle located at the tip of a nanotube which is bamboo-shaped as frequently observed. Both the HRTEM image and the corresponding electron diffraction pattern shown in Figure 7 are well consistent with a $\langle 110 \rangle$ projection of the cubic Co_9S_8 phase. Such multiwalled nanotubes partially filled with a cobalt sulfide were observed together with very abundant encapsulated nanoparticles which were found to be pure Co crystallites. Figure 8 presents the HRTEM image of a typical pure Co single-crystalline nanoparticle encapsulated in a few graphitic layers and surrounded by amorphous carbon. In this context, it is worth noting that we have found most of these cobalt nanoparticles in their high temperature f.c.c. phase; it was recently showed that this phase is not a consequence of rapid cooling in the growth process of such fine particles but is a stable phase for particles of this size [35]. Since the graphitic envelope provides an efficient protection against oxidation on their surface, the particles have a high crystallinity which enabled to perform the first magnetization measurements of individual ferromagnetic nanoparticles using high sensitive SQUID [5].

As far as nanotubes filled with rare earths are concerned, an extra difficulty in quantifying the elemental analysis is due to the fact that the S-$L_{2,3}$ edge is overlapping with the rare earth $N_{4,5}$ edge. Although it seems that in some cases, these nanowires also contain sulfur, a standard quantification method cannot be used and the chemical study requires further investigation. The HRTEM image in Figure 1d displays lattice periodicities which are well consistent with the structure of the DyS compound. In the case of Yb, the HRTEM image in Figure 1c would rather fit the cubic structure of pure Yb than that of YbS, but it should be noticed that these two compounds have close lattice periodicities.

Finally, another surprising result was observed for the nanowires obtained when the chosen element was S itself [31] (see Fig. 1e). In that case, unexpected high concentrations of Fe, which was the other major impurity of the graphite rods ($\approx 0.3\%$), were found along with S inside the nanotubes as shown in Figure 9. Thus the very abundant nanotubes formed on the cathode are filled with iron sulfides; in that case, iron probably played a crucial role as a metal for their formation.

All these results revealed an unexpected concentration phenomenon of sulfur inside numerous nanotubes (or iron in the particular case described above) although it was present as an impurity ($\approx 0.25\%$) in the graphite rods used for the arc-discharge experiments. They strongly suggest that three elements, *i.e.* carbon, a metal and sulfur, are involved in the growth mechanism of filled nanotubes. In order to confirm the crucial role of sulfur, further experiments described below were carried out using high purity carbon rods.

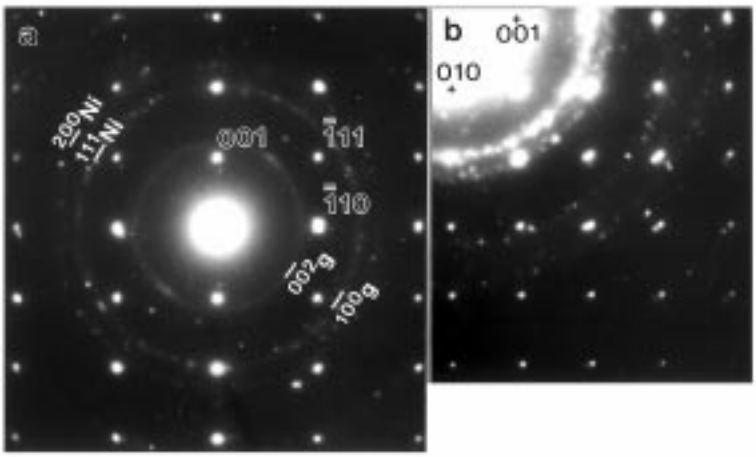

Fig. 6. (a) and (b) Selected area electron diffraction patterns of a conveniently oriented filled nanotube obtained with a 99.4% graphite anode doped with Ni. The structure is consistent with the pseudo-cubic Ni_3S_2 phase (rhombohedral cell: $a = 4.08$ Å, α close to 90°) which corresponds well to a S/Ni atomic ratio close to 0.7 observed in some EELS analyses. A $\langle 110 \rangle$ projection and a $\langle 100 \rangle$ projection can be seen in (a) and (b) respectively. The presence of numerous encapsulated nanoparticles in the selected area induces rings corresponding to reticular distances of the pure Ni phase (indicated by Ni) and of the graphitic structure (indicated by g) on the diffraction patterns.

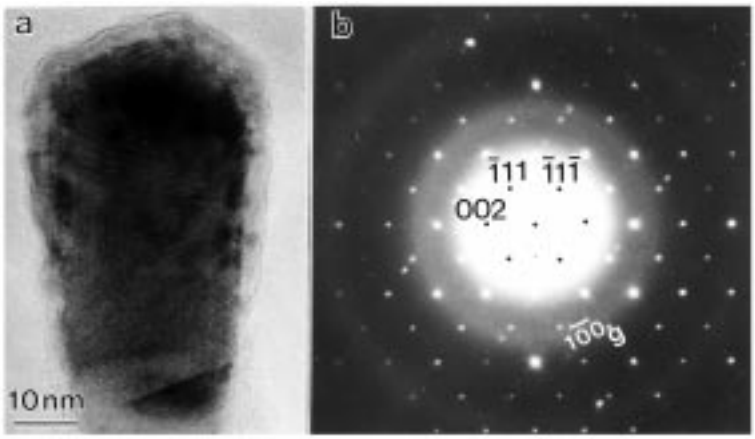

Fig. 7. HRTEM image in (a) and corresponding electron diffraction pattern in (b) of a conical particle at the tip of a bamboo-shaped carbon nanotube obtained with a 99.4% graphite anode doped with Co. Both are well consistent with a $\langle 110 \rangle$ projection of the cubic Co_9S_8 phase.

4 The key role of sulfur: the case of Cr filled nanotubes

We first tried to reproduce some of the experiments described in the previous section using high purity carbon rods (99.997%), the other experimental conditions being unchanged. High purity carbon rods were powdered to fill the anode along with the chosen element. We successively doped the anode with Cr (99.95%), Ni (99.9%), Co (99.9985%), Dy (99.9%) and S (sublimed) powders. Once the arc was established, the plasma was as stable as in previous experiments and a similar deposit was formed on the cathode. But the TEM observations of this deposit revealed that no filled nanotube could be found. For Ni and Co experiments, single-walled nanotubes (SWNT) similar to those usually observed in catalytic synthesis by arc-discharge [36] were obtained. Figure 10 shows SWNT produced with Ni: these nanotubes are very abundant and often self-organize in bundles that can exceed one micron in length. For Cr, Dy and S experiments, only a few empty multi-walled nanotubes could be found.

In order to confirm the crucial role of sulfur, we focused our attention on the case of Cr since the addition of this element produced the longest and most abundant encapsulated nanowires when using 99.4% graphite rods. Thus, we doped the anode with a mixture of Cr and S so that sulfur represents 0.1% in weight with respect to total C (*i.e.* drilled carbon anode and carbon powder inside). In these conditions, the atomic ratios are the following: S/C = 0.04%, Cr/C = 8% and S/Cr = 0.5% (1:200). This doping resulted in the formation on the cathode of numerous filled nanotubes, similar to those produced with 99.4% graphite rods. Although nanotubes completely filled from their tips are slightly less abundant, their length also often exceeds one micron as shown in Figure 11a and long single-crystals can be observed as previously (see Fig. 11b).

The chemical analysis of these nanowires revealed the existence of various compositions: some of them contain sulfur as those obtained previously (see Fig. 3), but most of them are free from sulfur and look like pure Cr nanowires encapsulated in graphitic shells and in some cases like chromium carbide encapsulated nanowires. Figure 12 presents a 3D plot of an EELS line-spectrum (64 spectra) acquired across a pure Cr filled nanotube (shown in inset) and the corresponding concentration profiles. C and Cr profiles are characteristic of a carbon nanotube whose hollow core is filled with Cr; the so-called S profile was deduced from the intensity in the S-$L_{2,3}$ edge energy-loss range and shows that no sulfur is detected. Finally, the concentration profiles obtained on a chromium carbide filled nanotube are presented in Figure 13. Here the C profile is not consistent with a nanotube having

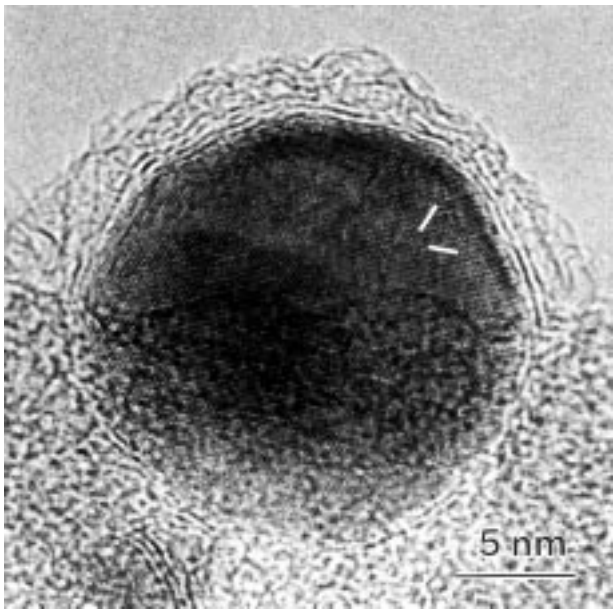

Fig. 8. HRTEM image of a typical pure Co single-crystalline nanoparticle obtained with a 99.4% graphite anode doped with Co. The particle is encapsulated in a few graphitic layers and surrounded by amorphous carbon. Such nanoparticles have mostly a face-centered cubic (f.c.c.) structure and often contain twin boundaries and stacking faults; these defects are known to frequently occur in this structure. The existence of elastic strains at the interface between the cobalt particle and the graphitic walls may be responsible for the observed distorsions in the f.c.c. structure. Here is the image of a nanoparticle almost in a $\langle 110 \rangle$ projection. The $\langle 111 \rangle$ dense atomic layers are indicated by small bars and separated by 2.0 Å. These HRTEM observations were performed using a Akashi 002B microscope.

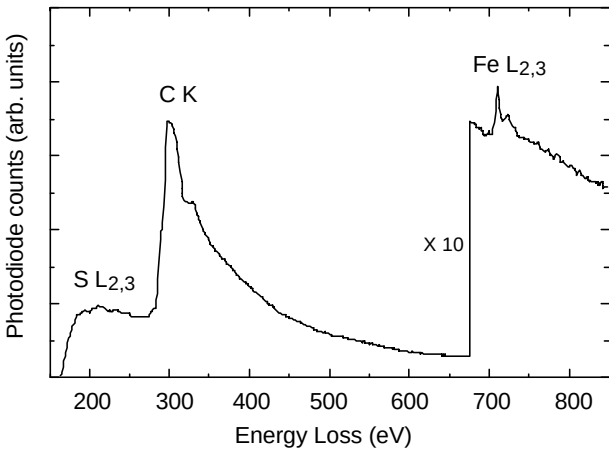

Fig. 9. Electron energy-loss spectrum after background subtraction obtained on a filled carbon nanotube obtained with a 99.4% graphite anode doped with S. Beside the C-K edge and the S-$L_{2,3}$ edge, the unexpected Fe-$L_{2,3}$ is present on the spectrum.

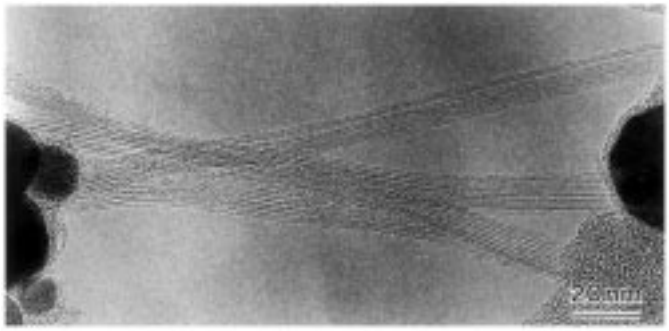

Fig. 10. TEM image of long bundles of single-walled nanotubes (SWNT) obtained when a high purity carbon anode was doped with Ni.

Fig. 11. (a) TEM image of a long typical filled carbon nanotube obtained with a high purity carbon anode doped with Cr and S in a S/Cr = 0.5% atomic ratio. (b) HRTEM image of another Cr-containing nanowire having a very small diameter and encapsulated in 10 graphitic layers. The filling is single-crystalline and in epitaxial relationship with the graphitic walls.

a carbon free hollow core. Moreover, the fine structure (ELNES) of the C-K edge in the core region is different from that in the peripheral region of the nanotube which is characteristic of graphitic walls as shown in the inset of Figure 13: the π^* peak is more intense and the overall shape of the σ^* band is modified.

No striking morphological difference was found between the different kinds of fillings. Note that the chemical composition may change along the nanotube and longitudinal line-spectra over the entire length of the fillings would be necessary to obtain good statistics. An investigation using the approach mentioned above, *i.e.* combining EELS analysis and electron diffraction on the same nanowire, is in progress in order to associate the chemical composition to the crystallographic structure of the filling material. It is already possible to state that the structure of numerous S containing nanowires is consistent with a trigonal chromium sulfide like Cr_5S_6 previously obtained for the nanowires produced with the 99.4% graphite rods. Moreover, many S free nanowires have a structure

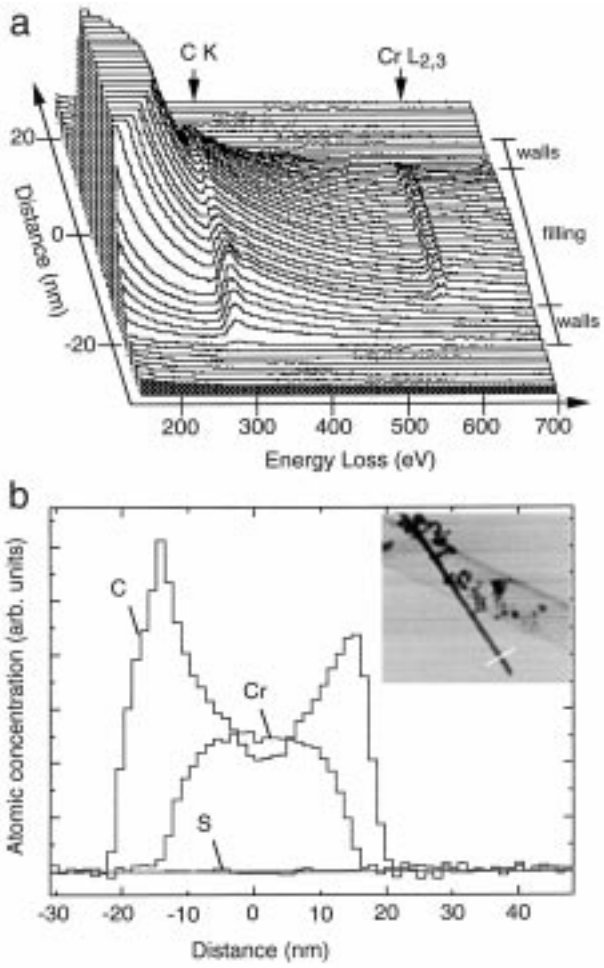

Fig. 12. Electron energy-loss line-spectrum across a pure Cr filled carbon nanotube obtained with a high purity carbon anode doped with Cr and S in a S/Cr = 0.5% atomic ratio. (a) 3D plot of the collection of 64 spectra acquired over 80 nm, showing the evolution of the C-K and Cr-$L_{2,3}$ edges as the electron beam scanned across the graphitic walls, the filling and again the graphitic walls. (b) Corresponding C and Cr concentration profiles. The so-called S profile is deduced from the intensity in the S-$L_{2,3}$ edge energy-loss range and shows the absence of sulfur. Inset: Bright field image of the nanowire.

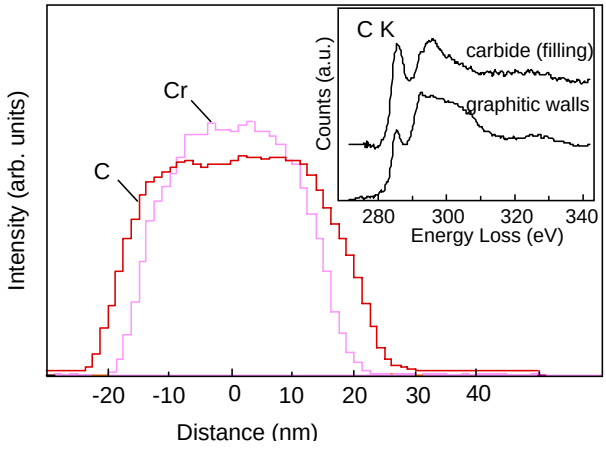

Fig. 13. Electron energy-loss line-spectrum across a carbon nanotube filled with a chromium carbide obtained with a high purity carbon anode doped with Cr and S in a S/Cr = 0.5% atomic ratio. The C concentration profile shows that the hollow core of the nanotube contains carbon in addition to Cr. Inset: ELNES structures of the C-K edge in the carbide core and on the sides, *i.e.* the graphitic walls of the nanotube.

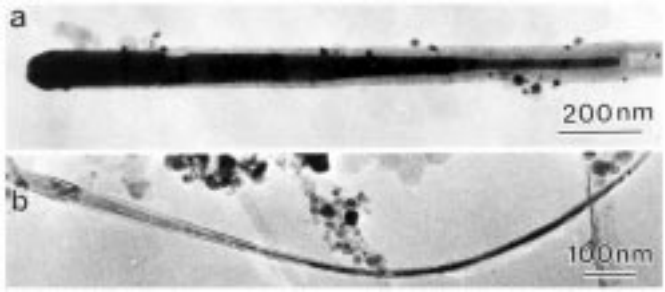

Fig. 14. (a) TEM image of a filled nanotube obtained with a 99.4% graphite anode doped with Ni, having a typical widened shape and a faceted tip. (b) TEM image of a several microns long filled nanotube, obtained with a high purity carbon anode doped with Cr and S in a S/Cr=0.5% atomic ratio, also having a slightly widened shape.

consistent with the orthorhombic Cr_3C_2 carbide. However, the structural identification of the nanowires which are pure Cr fillings according to EELS profiles requires further experiments since neither the b.c.c. Cr phase nor a A15 metastable Cr phase [37] could be unambiguously identified. As a conclusion, we have shown that the addition of a very small amount of sulfur to Cr provokes the formation of long encapsulated nanowires having various chemical compositions, including pure Cr.

5 Discussion

Our experimental results clearly show that sulfur is essential for the production of nanotubes filled with a large variety of materials. It is worth mentioning that the results with cobalt are very similar to those obtained by Kiang *et al.* [38,39]. They doped the anode with an equiatomic mixture of cobalt and sulfur to study the effect of sulfur on the production of SWNT and observed the formation of multiwalled nanotubes partially filled with a cobalt sulfide.

In contrast with other synthesis methods, it is likely that, according to the micronic length of numerous encapsulated nanowires, the nanotube and its filling form almost simultaneously: the filling by capillarity of empty nanotubes after their formation on the cathode is difficult to envisage on such a length and the variety of structural characteristics depending on the chosen element confirms this assumption. Furthermore, numerous filled nanotubes share striking similarities with catalytically grown carbon nanofibers [40,41]. The conical shape of Co containing elongated particles at the end of nanotubes (Fig. 7a) as well as the widened shape of long Ni or Cr containing nanowires shown in Figure 14 are representative features

reminding us of catalytically grown fibers. The catalytic growth mechanism of the latter may therefore give clues for the growth of filled nanotubes as already proposed by different authors [27,30].

In brief, we recall that nanofibers are usually obtained by catalytic decomposition of hydrocarbons (or carbon monoxide) on metal particles such as Fe, Co or Ni around 600 °C and can sometimes be partially filled by metallic carbide particles [42]. Growth models are based on three steps [43]: the hydrocarbon is first adsorbed on the metal surface and decomposed to produce carbon species which then dissolve and diffuse through the metallic particle and finally precipitate at the rear face of the particle to form the nanofiber. Different models were then proposed to explain the formation of hollow structures (see *e.g.* [44]). Moreover, the addition of sulfur was found to enhance the catalytic activity of cobalt [45]: it was claimed that the presence of small amounts of S promotes the reconstruction of the metal surface by giving a more favorable crystallographic orientation for the catalytic adsorption. Higher sulfur coverages give rise to a loss of the catalyst activity and in severe conditions, the bulk sulfide Co_9S_8 is formed as in electric arc experiments.

In spite of morphological similarities, carbon nanofibers and filled nanotubes are formed in different experimental conditions as far as temperature and species supply are concerned. In this respect, temperature is an essential parameter. In our experiments, filled nanotubes are found in localized regions of the soot around the cathode which depend on the chosen metal. This means that they grow on the cathode in a definite temperature range, in contrast with the vapor-phase self-assembled carbon nanomaterials (see *e.g.* [36]). We believe that in the electric arc experiment, one of the key factors is the important temperature gradient on the cathode which is created by the efficient water-cooling of the electrodes. Between the electrodes, a high temperature regime, probably above 4000 °C (*i.e.* above sublimation temperature of graphite) is responsible for the formation without any catalyst of the multiwalled carbon nanotubes discovered by Iijima [1]. On the rear part of the cathode, we assume that the temperature is lower than 1000 °C thanks to the water-cooling. Thus, we suggest that the temperature of formation of filled nanotubes ranges between 1000 °C and 2000 °C.

It is worth noting that the melting point of numerous metals belongs to this temperature range. We therefore suggest that the growth mechanism of nanotubes filled with metals in presence of sulfur follows a catalytic process, apart from the fact that the catalyst particle is in a molten state. In such a way, the catalyst material can flow inside the tube and fill it as it grows. Such a mechanism involving a molten catalyst particle has already been proposed to explain the rapid formation of carbon nanofibers, probably due to an increased diffusion rate of carbon in the liquid particle [46]. Zhang *et al.* proposed that the deposition and surface diffusion of carbon on a liquid-like metal is responsible for the formation of iron-filled nanotubules in their carbon arc in presence of $Fe(CO)_5$ gas [47]. In our case, we believe that the solid or molten state of the catalyst particle makes the difference between filled tubes and tubes capped by a metallic particle. Moreover the liquid state of the filling material during the growth seems essential to explain the various chemical compositions of the nanowires after solidification, as discussed later.

The specific role of sulfur in this catalytic process has to be discussed. Our results show that this element is crucial to obtain metal-based nanowires and is highly concentrated within a large number of them. S is not a catalyst in itself. However, it is known to promote below 2000 °C the graphitization of carbon materials, such as heavy petroleum products [48–50], by acting as a cross-linker and being then released from the graphitizing structure. We suggest that the same phenomenon occurs here. Therefore, we assume that C and S easily combine in the vapor phase at high temperature, maybe forming S-rich carbon clusters which would provide important amounts of S to the growing nanotube. Then, sulfur assists the graphitization of the nanotube on the cathode and helps the catalytic action of the metal. Finally S is released from the graphitizing tube and trapped in the metallic filling inside the nanotube because of its strong affinity with metals. This process results in a progressive increase of the S concentration in the nanowire. It gives an explanation for the difference in S concentration between the pure Co nanoparticles and the Co sulfide fillings of nanotubes: the final S amount in the filling material seems proportional to the final C amount, *i.e.* to the length of the nanotube. In addition, this sulfur concentration phenomenon certainly contributes to maintain the metallic material inside the growing nanotube in a molten state. Indeed, according to the Ni-S phase diagram for instance [51], the melting point decreases as the S concentration increases in the Ni-rich region. Finally, the spreading and wetting properties of the metallic phase over the graphitic walls can also be affected by the presence of sulfur.

The general scheme of the catalytic growth model we propose is sketched in Figure 15. The multiwalled nanotube starts to grow from a carbon-rich metal particle deposited on the cathode. Sulfur helps the precipitation of carbon and is then removed from the graphitizing walls. It is trapped by the metallic material and contributes to maintain it in a liquid state. In the same time, the S-enriched liquid flows inside the carbon nanotube. The growth will continue as long as the carbon, metal and sulfur species supply and temperature conditions will be maintained. Afterwards, during the solidification of the filling material, the cooling conditions will influence the microstructure of the final encapsulated nanocrystals. A rapid solidification will probably lead to the formation of numerous microcrystallites (see for instance Fig. 1f); on the contrary, if a solidification front can be established, the formation of long single-crystals in epitaxial relationship with the graphitic walls will be possible. Since sulfur is generally not soluble in metals, we believe that segregation phenomena occur at the solid-liquid interface as the solidification front moves through the nanowire: as a result, a pure metal crystal will grow and the S concentration

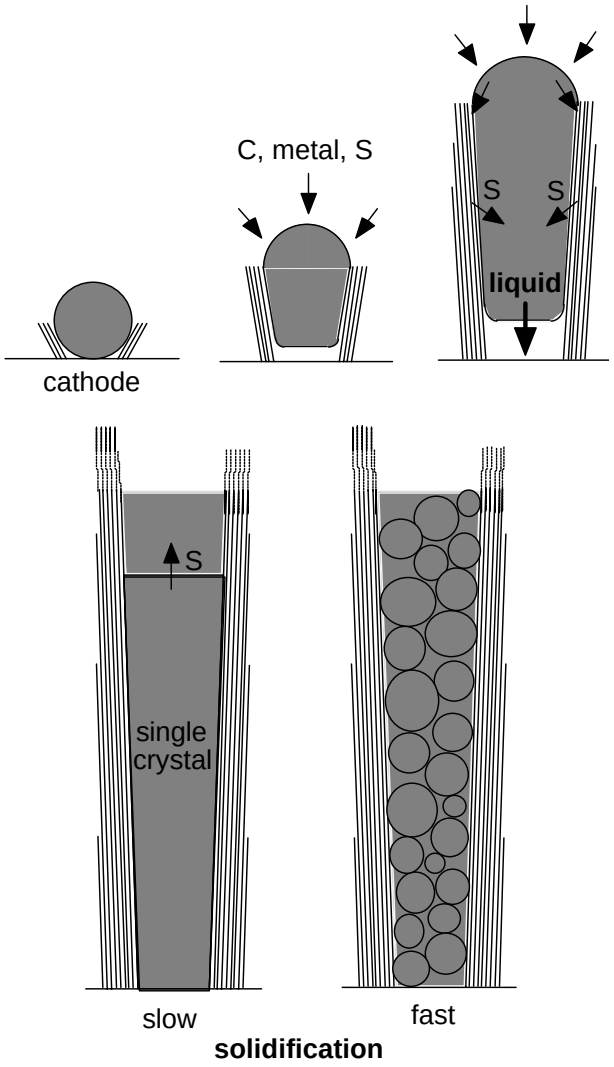

Fig. 15. Schematic growth mechanism proposed for the formation of a carbon nanotube filled with a metal on the cathode of an arc-discharge experiment in presence of sulfur (see text for details).

of the liquid phase will increase until the growth of a definite sulfide crystal replaces that of the pure metal. This is typically the case of Ni containing nanowires: longitudinal EELS analyses evidenced the coexistence of pure Ni crystals and Ni sulfides crystals inside the same nanotube. As far as the long pure Cr nanowires are concerned, we believe that their formation is due to the existence of a miscibility gap in the molten state between a pure Cr liquid and an S-rich liquid in the Cr-S phase diagram [51]. Therefore, the cooling of these different liquids will lead to the formation either of pure Cr crystals or of CrS compounds. A similar explanation can be proposed for the formation of pure Ge nanowires we observed although Ge is not a metal. In that case, GeS compounds are probably not formed because the number of encapsulating carbon layers is too reduced and the length of the nanotubes too short to obtain sulfur rich liquid particles of Ge. In all cases it is important to remind that the nanometric size of the crystallites and the confined space of the nanotubes may allow the formation of unusual phases.

Finally it is interesting to compare the formation of filled tubes and that of SWNT. In the latter case, a catalyst like Co or Ni is clearly required otherwise the SWNT would spontaneously close into graphitic domes [52]. Different models involving a catalytic growth either in the vapor phase (see *e.g.* [53,54]) or on the surface of a catalyst particle [55] have been proposed. In contrast to the experiments with Co by Kiang *et al.* [39], the presence of sulfur in our experiments with Co and Ni seemed to poison the formation of SWNT: only a few of them emanating radially from metal particles were found on the colder parts of the cathode. Therefore, it seems that in presence of sulfur, both SWNT and filled nanotubes grow from metal particles. Sulfur probably plays a role in the vapor phase by modifying the species supply and thus promoting the growth of multiwalled filled nanotubes on the cathode instead of self-assembled SWNT.

6 Conclusion

In conclusion, we have shown that the presence of sulfur in catalytic quantity is crucial for the production by the electric arc method of abundant metal containing encapsulated nanowires which can be free from sulfur. The role of sulfur may be compared to that of hydrogen in the formation of pure Ge and Cu encapsulated nanowires [29]. High spatial resolution EELS was proved to be essential and particularly adapted for characterizing filled carbon nanotubes and understanding their formation. We propose that sulfur enhances the catalytic activity of the metal as far as graphitization is concerned and helps the filling materials to remain in the liquid state and to flow inside the growing nanotubes.

We are grateful to C. Ricolleau, G. Hug, A. Jouniaux, M. Armand for their assistance in certain experiments and to S. Bonnamy, F. Beguin and F. Willaime for useful and stimulating discussions.

References

1. S. Iijima, Nature **354**, 56 (1991).
2. M.R. Pederson, J.Q. Broughton, Phys. Rev. Lett. **69**, 2689 (1992).
3. P.M. Ajayan, S. Iijima, Nature **361**, 333 (1993).
4. S.J. Tans, M.H. Devoret, H. Dai, A. Thess, R.E. Smalley, L.J. Geerligs, C. Dekker, Nature **386**, 474 (1997).
5. W. Wernsdorfer, E. Bonet Orozco, K. Hasselbach, A. Benoit, B. Barbara, N. Demoncy, A. Loiseau, H. Pascard, D. Mailly, Phys. Rev. Lett. **78**, 1791 (1997).
6. E. Dujardin, T.W. Ebbesen, H. Hiura, K. Tanigaki, Science **265**, 1850 (1994).
7. P.M. Ajayan, T.W. Ebbesen, T. Ichihashi, S. Iijima, K. Tanigaki, H. Hiura, Nature **362**, 522 (1993).
8. P.M. Ajayan, O. Stéphan, Ph. Redlich, C. Colliex, Nature **375**, 564 (1995).

9. Y.K. Chen, M.L.H. Green, S.C. Tsang, Chem. Commun. 2489 (1996).
10. D. Ugarte, A. Châtelain, W.A. de Heer, Science **274**, 1897 (1996).
11. S.C. Tsang, Y.K. Chen, P.J.F. Harris, M.L.H. Green, Nature **372**, 159 (1994).
12. Y.K. Chen, A. Chu, J. Cook, M.L.H. Green, P.J.F. Harris, R. Heesom, M. Humphries, J. Sloan, S.C. Tsang, J.F.C. Turner, J. Mater. Chem. **7**, 545 (1997).
13. H. Dai, E.W. Wong, Y.Z. Lu, S. Fan, C.M. Lieber, Nature **375**, 769 (1995).
14. W.K. Hsu, M. Terrones, J.P. Hare, N. Grobert, H.W. Kroto, D.R.M. Walton, Proceedings of the International Winterschool on Electronic Properties of Novel Materials, *Molecular Nanostructures* (Kirchberg 1997) p. 381.
15. W. Krätschmer, L.D. Lamb, K. Foristopoulos, D.R. Huffman, Nature **347**, 354 (1990).
16. T.W. Ebbesen, P.M. Ajayan, Nature **358**, 220 (1992).
17. R.D. Johnson, M.S. de Vries, J. Salem, D.S. Bethune, C.S. Yannoni, Nature **355**, 239 (1992).
18. R.S. Ruoff, D.C. Lorents, B. Chan, R. Malhotra, S. Subramoney, Science **259**, 346 (1993).
19. M. Tomita, Y. Saito, T. Hayashi, Jap. J. Appl. Phys. **32**, L280 (1993).
20. S. Seraphin, D. Zhou, J.Jiao, J.C. Withers, R. Loufty, Nature **362**, 503 (1993).
21. S. Seraphin, D. Zhou, J.Jiao, J.C. Withers, R. Loufty, Appl. Phys. Lett. **63**, 2073 (1993).
22. J.M. Cowley, M. Liu, Micron **25**, 53 (1994).
23. S. Subramoney, R.S. Ruoff, D.C. Lorents, B. Chan, R. Malhotra, M.J. Dyer, K. Parvin, Carbon **32**, 507 (1994).
24. J.M. Cowley, M. Liu, Carbon **33**, 225 (1995).
25. J.M. Cowley, M. Liu, Carbon **33**, 749 (1995).
26. Y. Saito, T. Yoshikawa, J. Crystal Growth **134**, 154 (1993).
27. P.M. Ajayan, C. Colliex, J.M. Lambert, P. Bernier, L. Barbedette, M. Tencé, O. Stéphan, Phys. Rev. Lett. **72**, 1722 (1994).
28. A.A. Setlur, J.M. Lauerhaas, J.Y. Dai, R.P.H. Chang, Appl. Phys. Lett. **69**, 345 (1996).
29. J.Y. Dai, J.M. Lauerhaas, A.A. Setlur, R.P.H. Chang, Chem. Phys. Lett. **258**, 547 (1996).
30. C. Guerret-Piécourt, Y. Le Bouar, A. Loiseau, H. Pascard, Nature **372**, 761 (1994).
31. A. Loiseau, H. Pascard, Chem. Phys. Lett. **256**, 246 (1996).
32. A. Loiseau, Full. Sci. Tech. **4**, 1263 (1996).
33. M. Tencé, M. Quartuccio, C. Colliex, Ultramicroscopy **58**, 42 (1995).
34. O. Stéphan, Ph.D. Thesis, Université d'Orsay, France (1996).
35. O. Kitakami, T. Sakurai, Y. Miyashita, Y. Takeno, Y. Shimada, H. Takano, H. Awano, Y. Sugita, Jpn J. Appl. Phys. **35**, 1724 (1996).
36. D.S. Bethune, C.H. Kiang, M.S. de Vries, G. Gorman, R. Savoy, J. Vasquez, R. Beyers, Nature **363**, 605 (1993).
37. K. Kimoto, I. Nishida, J. Phys. Soc. Jpn **22**, 744 (1967).
38. C.-H. Kiang, W.A. Goddard III, R. Beyers, J.R. Salem, D.S. Bethune, J. Phys. Chem. **98**, 6612 (1994).
39. C.-H. Kiang, M.S. Dresselhaus, R. Beyers, D.S. Bethune, Chem. Phys. Lett. **259**, 41 (1996).
40. N.M. Rodriguez, J. Mater. Res. **8**, 3233 (1993).
41. M.S. Dresselhaus, G. Dresselhaus, K. Sugihara, I.L. Spain, H.A. Goldberg in *Graphite Fibers and Filaments*, edited by M. Cardona (Springer, 1988).
42. M. Audier, A. Oberlin, M. Coulon, J. Cryst. Growth **55**, 549 (1981).
43. R.T.K. Baker, M.A. Barber, P.S. Harris, F.S. Feates, R.J. Waite, J. Catal. **26**, 51 (1972).
44. G.G. Tibbets, J. Cryst. Growth **66**, 632 (1984).
45. M.S. Kim, N.M. Rodriguez, R.T.K. Baker, J. Catal. **143**, 449 (1993).
46. F. Benissad, P. Gadelle, M. Coulon, L. Bonnetain, Carbon **26**, 425 (1988).
47. G.L. Zhang, F. Ambe, E.H. du Marchie Van Voorthuysen, L. Niesen, K. Szymanski, J. Appl. Phys. **80**, 579 (1996).
48. A. Oberlin, Carbon **22**, 521 (1984).
49. E. Fitzer, S. Weisenburger, Carbon **14**, 195 (1976).
50. X. Bourrat, A. Oberlin, J.C. Escalier, Fuel **542**, 521 (1987).
51. *Binary Alloy Phase Diagrams*, edited by T.B. Massalski (ASM International, 1990).
52. J.-C. Charlier, A. De Vita, X. Blase, R. Car, Science **275**, 646 (1997).
53. C.-H. Kiang, W.A. Goddard III, Phys. Rev. Lett. **76**, 2515 (1996).
54. A. Thess, R. Lee, P. Nikolaev, H. Dai, P. Petit, J. Robert, C. Xu, Y. Hee Lee, S. Gon Kim, A.G. Rinzler, D.T. Colbert, G.E. Scuseria, D. Tomanek, J.E. Fischer, R.E. Smalley, Science **273**, 483 (1996).
55. A. Maiti, C.J. Brabec, J. Bernholc, Phys. Rev. B **55**, R6097 (1997).